

# Different Approaches to Optimize High-Definition Matrix Headlights to Improve Computer Vision

Mirko Waldner, Nathalie Müller and Torsten Bertram

Institute of Control Theory and Systems Engineering (RST), TU Dortmund University, Germany

mirko.waldner@tu-dortmund.de

## Abstract

The contribution at hand presents and compares different online optimization approaches of dynamic illumination of matrix headlamps to improve automatic object recognition by neural networks. The approaches optimize, on the one hand, the network confidence and, on the other hand, the brightness of the image, the Weber contrast, and the gradient distribution on the image depending on the headlight beam pattern. The evaluation shows no objectively seen best cost function for the scenario studied, and selecting a cost function is a subjective decision. Optimizing the beam pattern to increase the confidence and intersection over union leads to inhomogeneous and subjectively disturbing beam patterns, and using contrast and gradient leads to similar results.

**Index Terms:** Matrix Headlight, Automated Driving, Optimization

## 1 Introduction

Automated object detection of traffic objects such as vehicles and pedestrians by computer vision, e.g., with neural networks, is similar to human perception but differs in some aspects, such as the dependence between the contrast of the object to its background and the resulting detection quality [1]. Previous studies have shown that higher contrast caused by stronger illumination of matrix headlights can reduce the quality of automatic recognition by computer vision [1]. Another aspect is that, unlike humans, a detection algorithm can communicate its confidence in the detected objects to the matrix headlight control algorithm faster than humans, enabling online illumination optimizations to maximize recognition quality with minimal energy consumption. Therefore, the different characteristics of automated computer vision and human vision require different and novel offline and online optimization approaches for the dynamic illumination of automotive matrix headlights to maximize traffic safety and system efficiency [2].



An automatic object detection neural network approach, e.g., YOLOv8 [3], has four main outputs: the predicted class of the object, the confidence of this classification, and the size and position of the enclosing bounding box. Fig. 1 shows an example of object detection in a virtual model of the German city of Lippstadt. In offline optimization, as presented in [4], the ground truth properties, e.g., the best bounding box, of the traffic objects are known, and a beam pattern can be optimized for neural networks by minimizing the error between reality and network output. However, in online optimization of dynamic illumination, the ground truth information is missing while driving, so the Generalized Intersection over Union (GioU) [5] and a control error cannot be computed. This paper focuses on the online case.

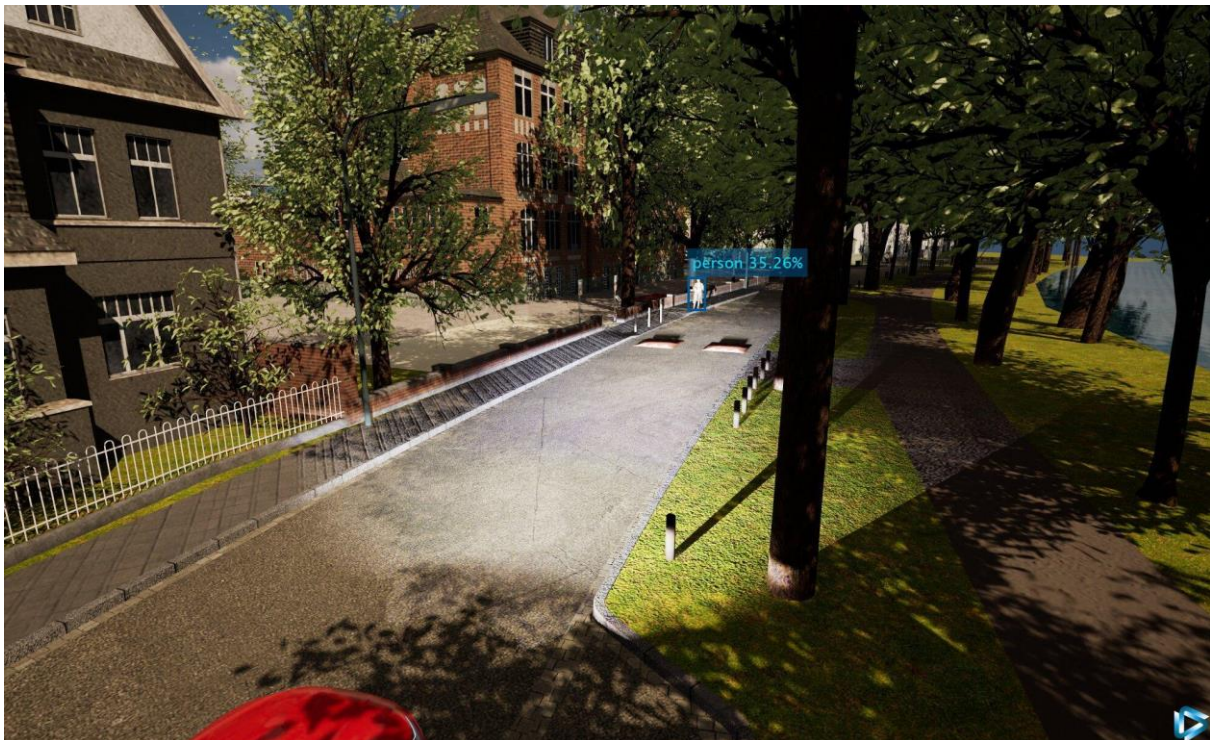


Figure 1: Automated detection of a pedestrian by the YOLOv8 [3] network in a virtual model of the German city of Lippstadt. The object class, confidence and bounding box are shown in blue. The ambient light is day-like only for this image and the ego-vehicle has a normal city light activated. In addition, the pedestrian is marked with a special light beam to remove his camouflage and improve the poor visibility due to the shadows of the leaves.

This contribution presents different novel online optimization approaches, mainly cost functions for high-definition (HD) matrix headlights, and the results are shown and compared. For this purpose, the optimization process is explained in the next chapter, and the possible cost functions are presented. The following evaluation chapter compares the different approaches based on the scenario shown in Fig. 1. A summary and an outlook conclude this paper.

## 2 Online Optimization of HD Matrix Headlights

One approach to optimize matrix headlights for computer vision is using the provided object detection quantities in a feedback loop. For the online case, this quantity is only the confidence and not the amount of overlap of the true and predicted bounding boxes. Therefore, a possible online optimization function would be to maximize the average confidence of all detected traffic objects [6]. The optimizer chooses the headlight parameters  $\mathbf{x} \in \mathbb{R}_{\geq 0 \wedge \leq 1}^{n_p}$ , which are the utilizations of the  $n_p$  individual light sources called pixels to minimize the cost function. If  $c_i(\mathbf{x}) \in \mathbb{R}_{\geq 0 \wedge \leq 1}$  is the confidence of the  $i$ -th object and  $n_o$  objects are detected, then the optimization task is to

$$\min_{\mathbf{x}} 1 - \frac{1}{n_o} \sum_{i=0}^{n_o-1} c_i(\mathbf{x}). \quad (1)$$

The advantage of this approach is that calculating the cost value is relatively simple and fast. However, the disadvantage is that the parts of the light distributions that do not illuminate the object and its background and thus do not contribute to its detection are not directly evaluated. Thus, the utilizations of pixels that do not emit light in the objects' direction are irrelevant and can, in principle, be arbitrary. This definition or cost gap can be solved by adding additional terms to (1), such as the energy consumption of the headlamp [6], but this leads to a weighted trade-off between the different aspects, e.g., best detection quality and minimal energy consumption, and can lead to unexpected results, such as the non-illumination of a pedestrian when the weights are set incorrectly.

Another approach is not using the detection results but the camera's color image to calculate the cost value. This method considers the entire beam pattern and is a kind of automatic camera image adjustment by the matrix headlight. The problem is that an HD matrix headlight can simply project the optimal image onto objects that minimize the cost function but do not improve visibility. For example, the scene could consist of only one wall, and the task is to maximize the edges in the image. In that case, the matrix headlamp will likely project a bright checkerboard rather than the optimal dimmed and homogeneous illumination that could make the wall's imperfections visible. The presented solution uses the grayscale image  $\mathbf{I} \in \mathbb{R}_{\geq 0 \wedge \leq 1}^{r_1 \times c_1}$  with  $r_1$  rows and  $c_1$  columns from the color image of the camera and compares it with all  $i$ -th intensity distributions  $\mathbf{I}_{v,i} \in \mathbb{R}_{\geq 0 \wedge \leq 1}^{r_2 \times c_2}$  with  $r_2$  rows and  $c_2$  columns from all  $n_m$  light modules of the ego vehicle. The intensity distributions  $\mathbf{I}_{v,i}$  of the  $i$ -th module is normalized to its intensity maximum  $I_{v,\text{Max},i}$  of this module to make it comparable with the grayscale image. The comparison is made by applying the same criteria function  $f(\mathbf{I}), f(\mathbf{I}_{v,i})$  to  $\mathbf{I}$  and  $\mathbf{I}_{v,i}$ , and calculating the difference or quotient of the results. This contribution uses division because it is easier for the authors to compare the course of the different cost functions. However, the influence of the choice between subtraction and division

was not further investigated. The general optimization task in this contribution is, with on the parameter vector  $x$  depending  $I$  and  $I_{v,i}$ , to

$$\min_x 1 - \frac{n_m f(I(x))}{\sum_{i=0}^{n_m-1} f(I_{v,i}(x))}. \quad (2)$$

The criterion function involves averaging over all rows and columns, so  $I$  and  $I_{v,i}$  can have a different resolution and number of texture elements (texels). In this contribution, an image pixel is called texel to avoid confusion with the matrix light sources. The complete optimization loop for both approaches is shown in Fig. 2.

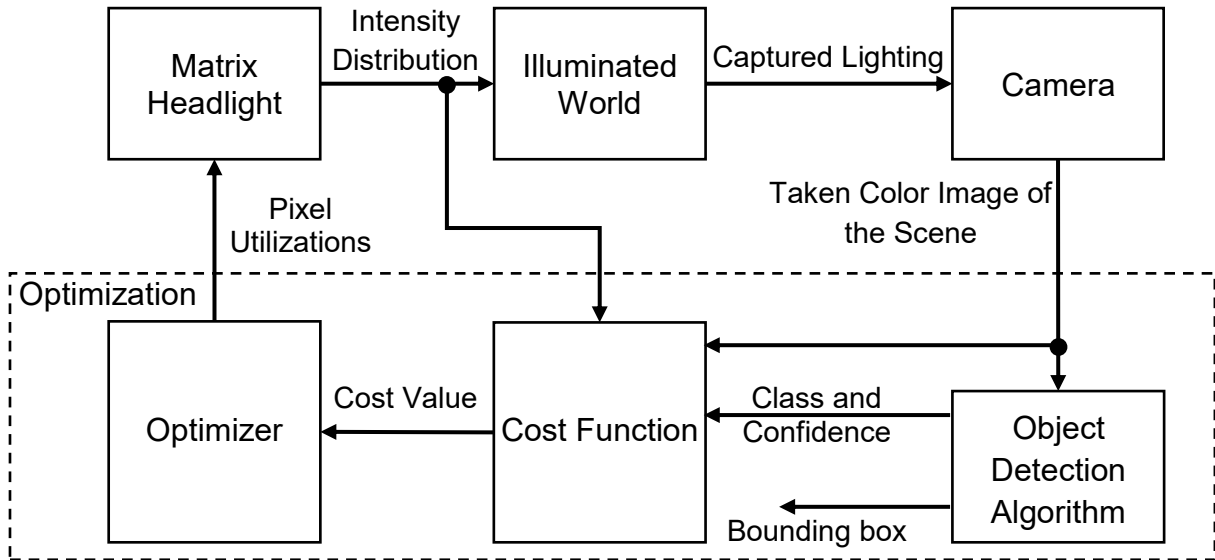


Figure 2: Online optimization loop of the illumination of the matrix headlamp.

Different approaches are possible for the formulation of  $f(I)$ . Since  $I$  and  $I_{v,i}$  have the same number type and range of values,  $f(I)$  will be formulated only for  $I$  in the following but can also be used for  $I_{v,i}$ . This contribution presents three main ideas: Analyzing the image directly, computing and measuring the Weber contrast [7], and computing and analyzing the image's gradients as a quantity for edge sharpness and homogeneity [8]. The Weber contrast  $t_{c,i,j}$  of the texel  $t_{i,j} \in \mathbb{R}_{\geq 0 \wedge \leq 1}$  of the  $i$ -th row and  $j$ -th column of  $I$  is

$$t_{c,i,j} = \frac{t_{i,j} - t_{B,i,j}}{t_{B,i,j}}, \quad (3)$$

where  $t_{B,i,j} \in \mathbb{R}_{>0 \wedge \leq 1}$  is the background of  $t_{i,j}$ , more precisely, the average value of the texels surrounding it. It is ensured that  $t_{B,i,j}$  is always  $> 0$  to avoid divisions by zero.  $t_{B,i,j}$  can be calculated by the discrete convolution of  $I$  with the kernel  $K_B \in \mathbb{R}^{3 \times 3}$  as  $t_{B,i,j} = (K_B * I)[i,j]$  with zero padding around the image. To obtain the background, the kernel is

$$\mathbf{K}_B = \frac{1}{8} \begin{bmatrix} 1 & 1 & 1 \\ 1 & 0 & 1 \\ 1 & 1 & 1 \end{bmatrix}. \quad (4)$$

The horizontal and vertical gradients  $t_{GH,i,j} = (\mathbf{K}_H * \mathbf{I})[i,j]$  and  $t_{GV,i,j} = (\mathbf{K}_V * \mathbf{I})[i,j]$  of the  $i$ -th row and  $j$ -th column can also be calculated using discrete convolution and the Sobel operators [9]  $\mathbf{K}_H \in \mathbb{R}^{3 \times 3}$  and  $\mathbf{K}_V \in \mathbb{R}^{3 \times 3}$ , which are

$$\mathbf{K}_H = \begin{bmatrix} 1 & 0 & -1 \\ 2 & 0 & -2 \\ 1 & 0 & -1 \end{bmatrix} \text{ and } \mathbf{K}_V = \begin{bmatrix} 1 & 2 & 1 \\ 0 & 0 & 0 \\ -1 & -2 & -1 \end{bmatrix}. \quad (5)$$

The overall gradient  $t_{G,i,j}$  of the  $i$ -th row and  $j$ -th column is

$$t_{G,i,j} = \sqrt{t_{GH,i,j}^2 + t_{GV,i,j}^2}. \quad (6)$$

Both gradient and contrast are considered possible optimization criteria because they differ for relevant situations. Two of these interesting situations are, for example, a texel surrounded by eight identical texels and uniformly increasing values such as

$$\mathbf{I}_{E1} = \begin{bmatrix} 0.1 & 0.1 & 0.1 \\ 0.1 & 1 & 0.1 \\ 0.1 & 0.1 & 0.1 \end{bmatrix} \text{ and } \mathbf{I}_{E2} = \begin{bmatrix} 1 & 2 & 3 \\ 1 & 2 & 3 \\ 1 & 2 & 3 \end{bmatrix}. \quad (7)$$

For the example  $\mathbf{I}_{E1}$ , the contrast is  $\frac{1-0.1}{0.1} = 9$  and the gradient 0, and for  $\mathbf{I}_{E2}$ , the contrast is  $\frac{2-2}{2} = 0$ , and the horizontal gradient is  $4 \cdot 1 - 4 \cdot 3 = -8$ . Since both quantities describe changes in brightness and lead to different values, both are considered as possible optimization criteria. The contrast is a kind of relative gradient. To illustrate the differences, Fig. 3 shows an image and the calculated contrasts and gradients of the same scene. One difference is that the lower right edge of the headlamp illumination is more visible in the contrast image than in the gradient image, but the roundness of the tree trunks is better seen at the gradients.



(a) Grayscale original image      (b) Grayscale absolute contrast      (c) Grayscale absolute gradient

Figure 3: Comparison of a grayscale image with its contrast and gradient distribution.

For the calculation of  $f(\mathbf{I}_{v,i})$  the entire  $\mathbf{I}_{v,i}$  is used, meaning that the outer texels of  $\mathbf{I}_{v,i}$  are all zero. This zero padding ensures that  $\mathbf{I}_{v,i}$  becomes brighter at higher intensities, and the outer contrast and gradient increase, even if the beam pattern is entirely homogeneous, so there is some energy consumption penalty in  $f(\mathbf{I}_{v,i})$ . For an entirely homogeneous beam pattern, the contrast and the gradients are close to zero so that a "good" [8] beam pattern leads to a small  $f(\mathbf{I}_{v,i})$ , which minimizes the costs of (2).

Several methods can reduce the captured grayscale image and its contrasts and gradients to a single value that can be used in (2). The individual  $t_{C,i,j}$  and  $t_{G,i,j}$  values themselves form an image with the same resolution  $r_1 \times c_1$  as  $I$ , but with possible values  $< 0$  and  $> 1$ . Therefore, the following reductions can be applied for all three cases, but for simplicity, the formulas are formulated only for  $t_{i,j}$ . One approach is calculating the mean absolute value of the image

$$\frac{1}{r_1 c_1} \sum_{i=0}^{r_1} \sum_{j=0}^{c_1} |t_{i,j}|. \quad (8)$$

The mean absolute value is close to zero for a homogeneous beam pattern due to the magnitude calculation for the contrast and gradient case. Another reduction approach is to calculate the variance of the image

$$\frac{1}{r_1 c_1} \sum_{i=0}^{r_1} \sum_{j=0}^{c_1} (t_{i,j} - \bar{t})^2 \quad \text{with} \quad \bar{t} = \frac{1}{r_1 c_1} \sum_{i=0}^{r_1} \sum_{j=0}^{c_1} t_{i,j}. \quad (9)$$

Both approaches yield zero as the minimum for a dark input image that occurs when the headlight is off. Using two reduction methods for the three approaches gives six different ways to calculate the cost value for (2). The possibility of mixing the calculations and using one scheme for the image and another for the intensity distribution of the module is not considered in this contribution.

### 3 Evaluation of the Usability of the Cost Functions

The quality of automatic object detection generally depends on the selected network and how the detection was learned. It also depends on the objects and the background. For example, we have experienced people of the same size but with different clothing, especially color, giving different results and leading to different confidence values. However, the general recognition behavior under different illumination levels has remained the same in previous studies [1]. Therefore, the course and relationship of the cost values to each other will change slightly for each test scenario or collection of scenarios.

The evaluation scenario chosen in this contribution is the detection of a pedestrian with the standard extra-large YOLOv8x [3] network from Ultralytics under urban environmental conditions. The YOLOv8 model is pretrained by Ultralytics on the COCO dataset, which consists mainly of daylight images. The model was not modified or explicitly trained for this contribution. Fig. 1 shows the daylight illumination scenario, and Fig. 4 shows the camera image for different headlight loads processed by the neural network. An in-house developed matrix headlight simulation based on Unreal Engine 5.1 called "See the Optimal Lighting" (SOL) [10] and its control algorithm [11] are used to generate the camera image, so the test scenario is virtual. The headlight has a horizontal beam angle of  $\pm 4^\circ$  and a vertical angle of  $-1^\circ$  (down) to  $3^\circ$  (up). The headlight has 16 columns and eight rows, and a pixel has a rectangular shape, a

homogeneous intensity distribution with a maximum intensity of 85,000 cd, and minimal overlap with its neighbors. Examples of the beam pattern can be seen in Fig. 6. The light color is entirely white. The virtual environment model is the Friedrichstraße in Lippstadt (GPS coordinates 51°40'35.7 "N 8°20'11.3 "E) measured and virtually modeled by 3D Mapping Solutions GmbH. The pedestrian is from the Twinmotion Posed Humans Winter Pack 1 by Epic Games. The ambient lighting is 0.3 lx, and the leaves of the trees shade the pedestrian. When the headlights of the ego-person vehicle are disabled, the neural network does not detect the pedestrian.



(a) 7 % Headlight utilization      (b) 26 % Headlight utilization      (c) 66 % Headlight utilization

Figure 4: Camera image for three different headlight utilizations. All pixels are set to the same relative power value, so that the resulting intensity distribution is homogeneous.

This contribution uses a two-step procedure to evaluate the different optimization criteria. In the first step, the intensity distribution of the headlamp is homogeneously changed from 0.01 % to 100 % of its maximum, i.e., all pixels are set to the same utilization value. The resulting beam pattern is almost perfectly homogeneous, with a minimal drop between the illumination of the pixels as in an ideal projector. The resulting behavior of the cost values is shown in Fig. 5. All curves are normalized to their maxima for better comparability, so zero is the minimum for all curves. The GloU [5] is the degree of overlap between the predicted bounding box of the pedestrian and a reference generated using the neural network to detect the object under daylight conditions. A GloU of 1 means a perfect match, 0.5 means 50 % overlap, and the GloU becomes more negative the farther apart the boxes are. To compare the GloU and confidence with the other novel cost functions, they are shown inverted in Fig. 5. Comparing the curves in Fig. 5, three subjectively interesting intervals appear. The first interval ranges from 5 % to 10 % utilization, where the one-minus confidence and GloU curves and the image and gradient variance cost functions have their minimum. As Fig. 4a shows, the pedestrian is clearly visible at this illumination level, and the background is dark. The next region is between 20 % and 30 % utilization, where the confidence and GloU curves do not change much, and the contrast and mean gradient cost functions have their minimum. Here, the person and the background are well illuminated (see Fig. 4b). The third interval begins at about 40 %, where the one minus confidence curve rises sharply. At this point, the scene's illumination is subjectively too intense (see Fig. 4c).

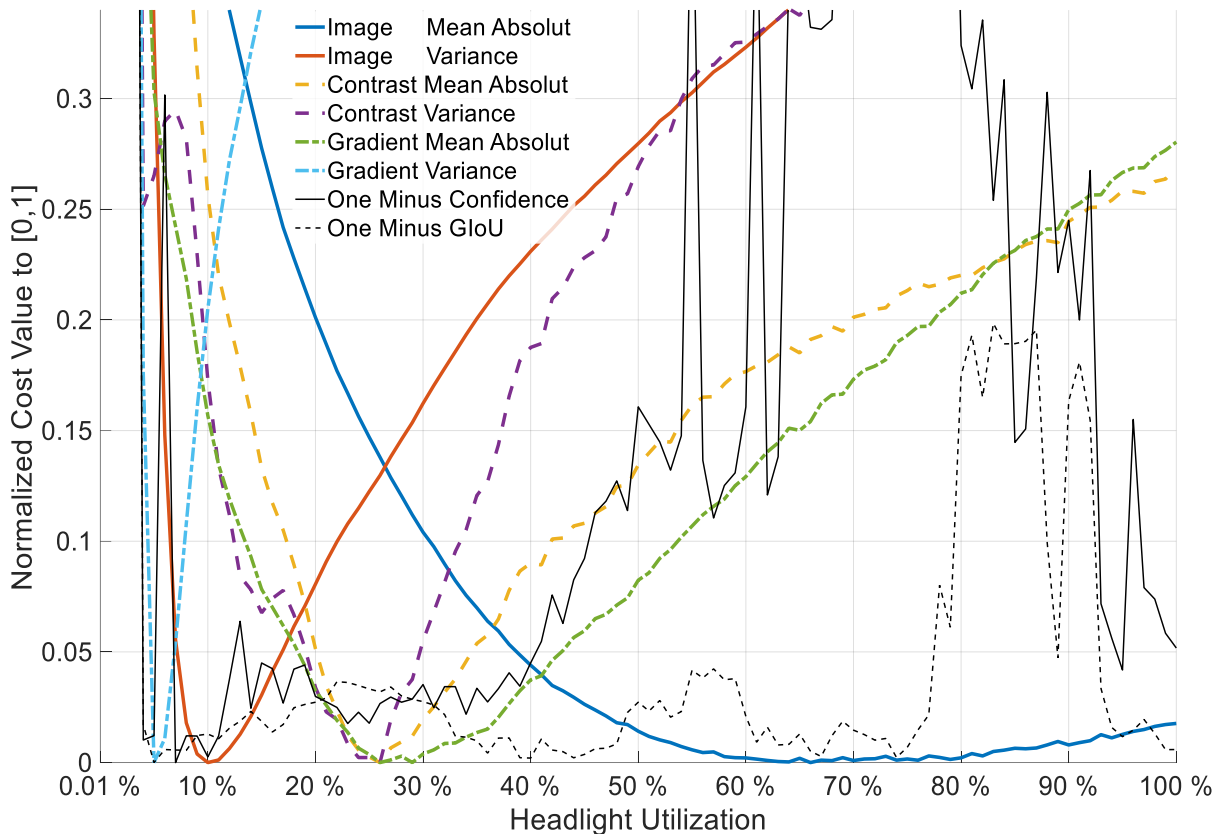


Figure 5: Comparison of the behavior of the colored cost functions and the one minus confidence and GloU curves in black for different headlight utilization rates.

In addition to comparing the curves, the root mean squared error (RMSE) between the cost function curves and the confidence and GloU curves was calculated and is shown in Table 1. According to the calculation, the mean absolute value of the gradient best matches the behavior of the confidence and GloU curves in this test case. However, the variance of the gradient is the worst.

Table 1: Calculation of the Root Mean Squared Error between the cost function curves and the confidence and GloU curve. All curves can be seen in Fig. 5.

| Criteria              | RMSE to Confidence Curve | RMSE to GloU Curve |
|-----------------------|--------------------------|--------------------|
| Image Mean Absolut    | 0.2591                   | 0.1820             |
| Image Variance        | 0.1759                   | 0.2638             |
| Contrast Mean Absolut | 0.1538                   | 0.1711             |
| Contrast Variance     | 0.1565                   | 0.2490             |
| Gradient Mean Absolut | <b>0.1375</b>            | <b>0.1306</b>      |
| Gradient Variance     | 0.4863                   | 0.5992             |

For the second evaluation, the Matlab particle swarm optimizer [12] is connected to the headlight simulation in Unreal Engine via shared-memory interprocess communication and performs the optimization tasks of (1) and (2). The particle swarm parameters have the default configuration. The lower bound of the parameters is  $> 0$ , the upper bound is one, and the initial population is 100 homogeneous illuminations from 0.01 % to 100 % for all cases. The optimization terminates when either 100 iterations have been performed, or the default criteria are met. In 62.5 % of the cases,



the optimization ends before 100 iterations, and the mean number of iterations required is 83.25. Without the warm start, the optimization would require more iterations. Preliminary research has shown that the warm start does not affect the optimal parameters but only reduces the processing time. The final image taken at the end of the optimization with the optimal parameters and the resulting intensity distribution are shown in Fig. 6.

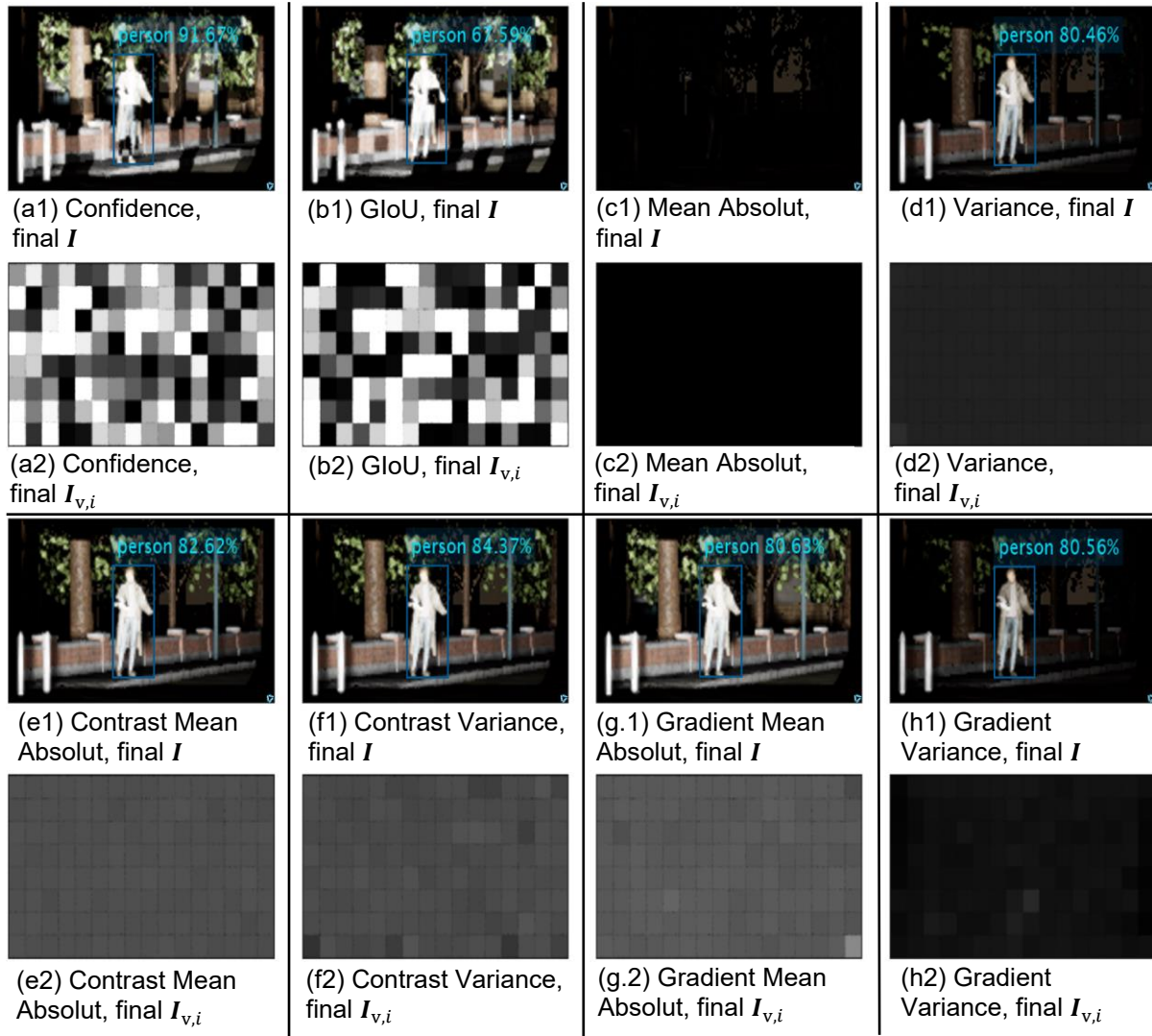


Figure 6: Comparison of final  $I$  and  $I_{v,1}$  stored after the optimization is finished. The grayscale intensity distributions shown are scaled to 75 % of the possible maximum. The mean utilization for all cases is, in order from (a) to (h), 44.00 %, 40.93 %, 0.00 %, 10.08 %, 23.38 %, 21.99 %, 26.46 %, and 4.84 %.

In the author's opinion, some interesting evaluation results exist, but no clear best cost function exists. The chaotic light distributions (see Figs. 6a2 and 6b2) after optimizing confidence and GloU support the argument from Chapter 2 that using these criteria alone does not result in a subjectively appealing and well-selling matrix headlight light distribution. Also, optimizing the GloU results in the lowest confidence of all cases when the person is detected. Using the mean absolute brightness relative to the brightness of the headlamp results in the optimizer turning off the headlamp so that

only the ambient light is visible in the image (see the house wall in the background of Fig. 6c1). This is because the mean absolute value of  $I_{v,i}$  approaches zero only when the headlight gets darker or is almost off, and the other variants can lead to values close to zero for a brighter headlight because the calculation depends on the mean value or the ratios of the pixel neighbors to each other. Therefore, this mean absolute image cost function is not valid. From an objective point of view, all remaining cost functions seem promising for further investigation because the differences in the RMSE in Table 1 and in the shape of the curves in Fig. 5 are too small for the authors. Optimization according to variance seems to result in a darker background and reduce the overexposure of the pedestrian in the foreground. At this point, the cost functions subjectively favored by the authors are the mean of absolute contrast (see Fig. 6e) and gradient (see Fig. 6g) since they have a subjectively good compromise between foreground and background illumination, resulting in homogeneous ray patterns with the lowest RMSEs.

## 4 Summary & Outlook

The contribution at hand has demonstrated several novel online optimization approaches for dynamic illumination of matrix headlights to improve automatic object recognition by neural networks. The approaches are maximizing the network's confidence, the image's brightness, and the Weber contrast and gradient distribution on the image concerning the headlight pattern. The evaluation shows no objectively seen best cost function in the evaluated scenario. Optimizing the beam pattern to increase the confidence and intersection over the union results in chaotic beam patterns. Using variance appears to result in a darker background, but it subjectively improves the visibility of the internal structure of foreground objects compared to the mean. Using the absolute mean and variance of contrast and slope seem promising for further research, and optimizing the mean brightness should be discarded as it resulted in a deactivated headlight.

In further research, the presented evaluation should be extended to a collection of test scenarios to understand better the behavior of the cost functions and optimization under different conditions. Furthermore, it is planned to consider not only the changes in the contrast level and gradient but also the changes in their direction when formulating the cost function.

## 5 Acknowledgment

All 3D environment objects, e.g. trees and houses, of this contribution, were created by 3D Mapping Solutions. This work is funded by the German Federal Ministry for Economic Affairs and Climate Action as part of the AHEAD project (grant number: 19A21021C), which is a collaboration with Forvia-Hella and 3D Mapping Solutions. The responsibility for the content of this publication lies with the authors.

## 6 References

- [1] M. Waldner, N. Müller and T. Bertram: Energy-Efficient Illumination by Matrix Headlamps for Nighttime Auto-mated Object Detection, International Journal of Electrical and Computer Engineering Research, Vol. 2 No. 3 (2022)
- [2] R. Kauschke, M. Waldner, N. Müller, T. Bertram and M. Grünke: Ist automatisiertes Fahren mit kamera-optimierten Lichtfunktionen besser möglich? Top-Down-Entwicklung optimierter Lichtverteilungen für das automatisierte Fahren, 9. VDI-Tagung Optische Technologien in der Fahrzeugtechnik 2022, 30.06.-01.07.2022
- [3] Ultralytics (Ed.): YOLOv8, <https://github.com/ultralytics/ultralytics>, 2023
- [4] D. Hoffmann, A. Erkan, T. Singer and T. Q. Khanh: Investigation of different influencing parameters on the quality of object detection by camera systems in highly automated vehicles, 14th International Symposium on Automotive Lighting (ISAL) 2021, 04.-06.04.2022
- [5] H. Rezatofighi, N. Tsoi, J. Gwak, A. Sadeghian, I. Reid and S. Savarese: Generalized Intersection over Union, The IEEE Conference on Computer Vision and Pattern Recognition (CVPR), June 2019
- [6] N. Müller, M. Waldner and T. Bertram: Virtual Development and Optimization of High-Definition Headlights, 2022 International Conference on Electrical, Computer, Communications and Mechatronics Engineering (ICECCME), 2022
- [7] E. Peli: Contrast in complex images, JOSA A 7.10, 1990
- [8] B. Wördenweber et al.: Automotive lighting and human vision. Vol. 1. Springer-Verlag Berlin Heidelberg, 2007
- [9] I. Sobel: An Isotropic 3x3 Image Gradient Operator, Presentation at Stanford A.I. Project 1968, 2014
- [10] M. Waldner and T. Bertram: Simulation of High-Definition Pixel-Headlights, 15th International Symposium (ISVC), 2020
- [11] M. Waldner and T. Bertram: Feedforward Control of HD-Headlights for Automated Driving, 14th International Symposium on Automotive Lighting (ISAL) 2021, 04.-06.04.2022
- [12] Mathworks (Ed.): Particle swarm optimization with the Matlab Global Optimization Toolbox, <https://de.mathworks.com/help/gads/particleswarm.html> , 2023